

# Stereoelectronic Features of the Cinchona Alkaloids Determine Their Differential Antimalarial Activity

Jean M. Karle\* and Apurba K. Bhattacharjee

Department of Pharmacology, Division of Experimental Therapeutics, Walter Reed Army Institute of Research, Washington, DC 20307, USA

Received 22 October 1998; accepted 28 December 1998

**Abstract**—For most potent antimalarial activity, the cinchona alkaloids appear to require certain electronic features, particularly a sufficiently acidic hydroxyl proton and an electric field direction pointing from the aliphatic nitrogen atom towards the quinoline ring. These observations are the result of an analysis of molecular electronic properties of eight cinchona alkaloids and an in vivo metabolite calculated using ab initio 3-21G quantum chemical methods in relation to their in vitro IC<sub>50</sub> values against chloroquine-sensitive and chloroquine-resistant *Plasmodium falciparum* parasites. The purpose is to provide a profile of the electronic characteristics necessary for potent antimalarial activity for use in the design of new antimalarial agents and to gain insight into the mechanistic path for antimalarial activity. Distinguishing features of the weakly active epiquinine and epiquinidine include a higher dipole moment, a different direction of the electric field, a greater intrinsic nucleophilicity, lower acidity of the hydroxyl proton, a lesser electron affinity of the lowest unoccupied molecular orbitals, and a higher proton affinity than the active cinchona alkaloids. A moderately potent quinine metabolite possesses some, but not all, of the same electronic features as the most potent cinchona alkaloids. Both the positioning of the hydroxyl and aliphatic amine groups and their electronic features appear to play a crucial role for antimalarial potency of the cinchona alkaloids, most likely by controlling the ability of these groups to form effective intermolecular hydrogen bonds. © 1999 Elsevier Science Ltd. All rights reserved.

## Introduction

The cinchona alkaloids (Fig. 1) are found in the bark of *Cinchona ledgeriana* Moens, which has been used directly or in the form of powders as a remedy for malaria ever since it was included in the 1677 edition of the *London Pharmacopoeia* as ‘Cotex Peruanus’.<sup>1</sup> Quinine remains the drug of choice for the treatment of multidrug-resistant *Plasmodium falciparum* malaria and cerebral malaria, except in Southeast Asia.<sup>2–4</sup> Although the parasite digestive vacuole appears to be the site of action of the cinchona alkaloids, the specific mechanism of antimalarial action of the cinchona alkaloids is still unclear.<sup>2,5,6</sup> The previously proposed theory of drug–DNA binding is no longer favored.<sup>2</sup> The extent to which alkalization of the parasite acid vesicles through accumulation of quinine or quinidine contributes to parasite death is also unclear.<sup>6,7</sup> Quinine has been shown to inhibit haem polymerase extracted from *Plasmodium falciparum* trophozoites which may play an important role in its antimalarial activity.<sup>8</sup>

Intrinsic molecular properties like dipole moment, electric field direction, molecular electrostatic potentials, and molecular orbital energies can provide a wealth of information for assessing molecular interactions when biological recognition processes are involved.<sup>9–12</sup> These electronic profiles can lead to direct inferences about the nature of the corresponding receptor site and about the interaction between these sites and an approaching drug molecule. Thus, to better understand the mechanism of action of the cinchona alkaloids in terms of the interaction of these alkaloids with receptor molecules, the present study was performed to assess the importance of specific molecular electronic properties with respect to antimalarial activity, to relate these properties to those of other aromatic carbinolamine antimalarial agents, and to explain why the configuration of the epi alkaloids greatly reduces their antimalarial activity.<sup>13</sup>

## Results and Discussion

### Optimized geometry of the cinchona alkaloids

The calculated optimized conformations (Fig. 2) of the free base forms of active *erythro* alkaloids (quinine, quinidine, dihydroquinine, dihydroquinidine, cinchonine,

Key words: Malaria; cinchona alkaloids; stereoelectronic properties; ab initio quantum mechanics.

\* Corresponding author. Tel.: +1-301-319-9633; fax: +1-301-319-9449; e-mail: jean.karle@na.amedd.army.mil

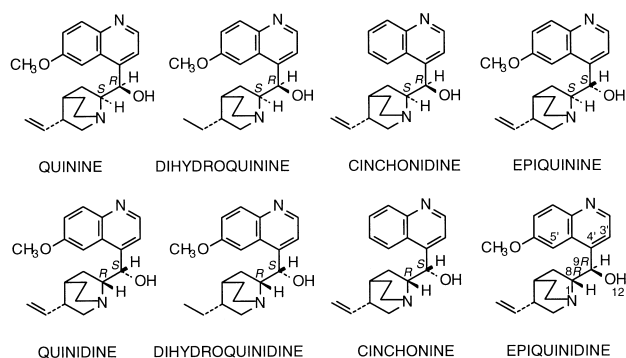


**Figure 1.** Chemical structures of the cinchona alkaloids. Each structure is labeled with the configuration of the C8 and C9 carbon atoms. The numbering scheme for selected atoms is shown on the epiquinidine structure.

and cinchonidine) and the inactive *threo* alkaloids epiquinine and epiquinidine differ in several significant ways. These differences result in the *threo* alkaloids having (i) a smaller distance between the aliphatic nitrogen atom N1 and the hydroxyl oxygen atom O12, (ii) a larger distance between N1 and the C5' atom of the quinoline ring, and (iii) a different orientation of the quinuclidine ring with respect to the quinoline ring as defined by the H8-C8-C9-H9 dihedral angle. For the *erythro* alkaloids, the N1...O12 distance equals 3.14 to 3.19 Å, the N1...C5' distance is around 3.9 Å, and the H8-C8-C9-H9 dihedral angle is either  $-79.2$  to  $-81.9^\circ$  or  $79.8$  to  $92.1^\circ$ . For the *threo* alkaloids, the N1...O12 distance is shorter at 2.82 to 2.89 Å, the N1...C5' distance is around 5.3 Å, and the H8-C8-C9-H9 dihedral angle is  $169.2$  to  $174.7^\circ$  corresponding to an anti arrangement of H8 and H9.

These optimized conformations are similar to and thus consistent with the conformations of the alkaloids found in crystal structures<sup>13–20</sup> and in solution as measured by NMR.<sup>21,22</sup> In the crystal structures, the H8-C8-C9-H9 dihedral angle for the *erythro* alkaloids is  $|61.2|$  to  $|83.9|^\circ$  and *threo* alkaloids is  $173.7$  to  $174.4^\circ$ . The crystalline N1...O12 distance is equal to 2.93 to

3.22 Å for the *erythro* alkaloids and 2.82 Å for the *threo* alkaloids. The dihedral angle C3'-C4'-C9-O12, which defines the orientation of the hydroxyl group with respect to the quinoline ring, is essentially the same as for the crystal structures and matches the NMR solution structure for those alkaloids whose orientation is given. The only exception is epiquinine whose calculated and crystalline C3'-C4'-C9-O12 dihedral angle differs by  $28^\circ$ . However, the calculated non-bonded distance between N1...C5' for both the *erythro* and *threo* alkaloids is within 0.4 Å of the crystal structures.

### Dipole moment

Both the direction and magnitude of the dipole moment of the inactive *threo* epi alkaloids and the active *erythro* alkaloids are distinctly different (Table 1). Epiquinine and epiquinidine have a dipole moment of 3.52 and 2.43 Debye, respectively, whereas the magnitude of the dipole moment for the *erythro* alkaloids is lower ranging from 1.02 to 2.20 Debye. In addition, the dipole moment in the *erythro* alkaloids points from the aliphatic nitrogen atom (positive end) towards the quinoline ring whereas the positive end of the dipole moment for the *threo* epi alkaloids is located away from the aliphatic nitrogen atom near either the middle of the quinuclidine ring or near the vinyl group (Fig. 2). Since the dipole orientation represents the direction of the electric field due to charge distribution and the dipole magnitude is directly related to the interaction energy with the electronic field surrounding an approaching molecule, the dipole moment and its direction are important for interpreting and predicting molecular reactivity.<sup>10,23</sup> Thus, the significantly greater polarization and the shift in the direction of the dipole moment in the epi alkaloids may be linked to their diminished potency.

### Molecular electrostatic potential

The color-coded plots in Figure 3 illustrate the electrostatic potential plotted onto essentially the van der Waals surface. For all of the alkaloids, the most positive potential (the deepest blue color) is located by the

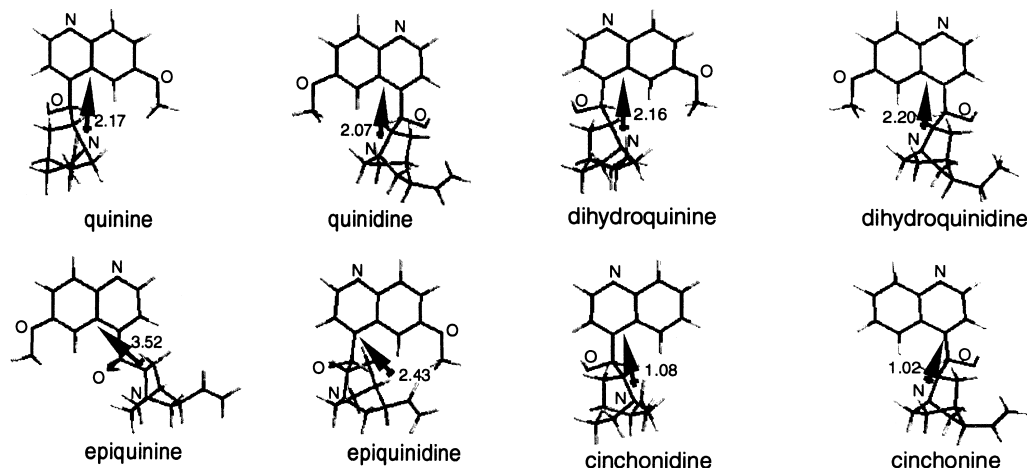


**Figure 2.** Optimized conformations of the cinchona alkaloids. The direction of the dipole moment is illustrated by the arrow with the bottom of the arrow indicating the positive end of the dipole. The magnitude of the dipole moment is given next to the arrow.

**Table 1.** Calculated electronic properties<sup>a</sup> and in vitro antimalarial activities

Cinchona alkaloid	Configuration	IC <sub>50</sub> D-6 clone (nmol)	IC <sub>50</sub> W-2 clone (nmol)	Dipole moment (Debye) and its direction <sup>b</sup>	Most negative potential (kcal/mol)	Negative potential by aliphatic N atom (kcal/mol)	Positive potential by aliphatic OH group <sup>c</sup> (kcal/mol)	HOMO (eV)	LUMO (eV)	Proton affinity (kcal/mol)
Quinine	<i>erythro</i>	29.3	103.2	2.17	−63.6	−58.6	35.1	−8.88	−0.55	195.6
Dihydroquinine	<i>erythro</i>	21.3	151.7	2.16	−64.2	−60.9	34.7	−8.87	−0.54	197.6
Quinidine	<i>erythro</i>	13.4	43.7	2.07	−64.3	−59.4	35.7	−8.88	−0.55	195.6
Dihydroquinidine	<i>erythro</i>	10.4	74.1	2.20	−64.2	−61.2	35.0	−8.87	−0.54	198.1
Cinchonine	<i>erythro</i>	18.3	70.8	1.02	−64.5	−64.4	35.3	−9.15	−0.56	203.2
Cinchonidine	<i>erythro</i>	69.5	206.8	1.08	−64.4	−62.9	34.9	−9.16	−0.57	203.3
Epiquinine	<i>threo</i>	3471.0	1179.0	3.52/	−65.6	−63.9	28.0	−8.67	−0.30	226.5
Epiquinidine	<i>threo</i>	2700.0	1024.0	2.43/	−82.7	−82.7	31.4	−8.68	−0.31	227.6
3'-Hydroxyquinine	<i>erythro</i>	123.0	— <sup>d</sup>	0.64/	−63.5	−61.8	25.4	−8.98	−0.65	198.8

<sup>a</sup> In an aqueous medium.<sup>b</sup> Symbol | signifies dipole moment pointing from the aliphatic nitrogen atom towards the quinoline ring. Symbol / signifies dipole moment angled away from the aliphatic nitrogen atom.<sup>c</sup> The aliphatic hydroxyl hydrogen atom is the site of the most positive potential except for 3'-hydroxyquinine in which the aromatic hydroxyl group is the site of the most positive potential.<sup>d</sup> Not determined.

hydroxyl proton, and the most negative potential (the deepest red color) is located by the quinoline nitrogen atom except for epiquinidine. The region adjacent to the aliphatic quinuclidine nitrogen atom is also highly negative and is the most negative potential site for epiquinidine. The molecular electrostatic potential of the active *erythro* alkaloids and the inactive *threo* epi alkaloids differs in several significant ways. A detailed analysis of these potentials, (Fig. 3, Table 1) shows that (i) the most negative potential in the inactive epi alkaloids is more negative than in the active *erythro* alkaloids, (ii) the negative potential located by the aliphatic nitrogen atom in the inactive epi alkaloids is also more negative than in the *erythro* alkaloids except for cinchonine, and (iii) the positive potential located by the hydroxyl proton in the epi alkaloids is less positive than in the *erythro* alkaloids. Thus, antimalarial potency is associated

with a most negative potential of −63.6 to −64.5 kcal/mol, a negative potential by the aliphatic nitrogen atom of −58.6 to −64.4 kcal/mol, and a positive potential of at least 34.7 kcal/mol. Since the positive and negative potentials are a measure of the intrinsic acidity and basicity respectively, of the hydroxyl and amine groups, the results indicate that for antimalarial activity the alkaloids should contain a hydroxyl group of sufficient acidity and quinoline and aliphatic nitrogen atoms that are not too basic.

Three-dimensional electrostatic potential surfaces at a constant value of −10 kcal/mol are illustrated in Figure 4, again showing differences between the *erythro* and *threo* alkaloids. The isopotential surfaces at −10 kcal/mol for quinine, quinidine, dihydroquinine, dihydroquinidine, cinchonine, and cinchonidine have

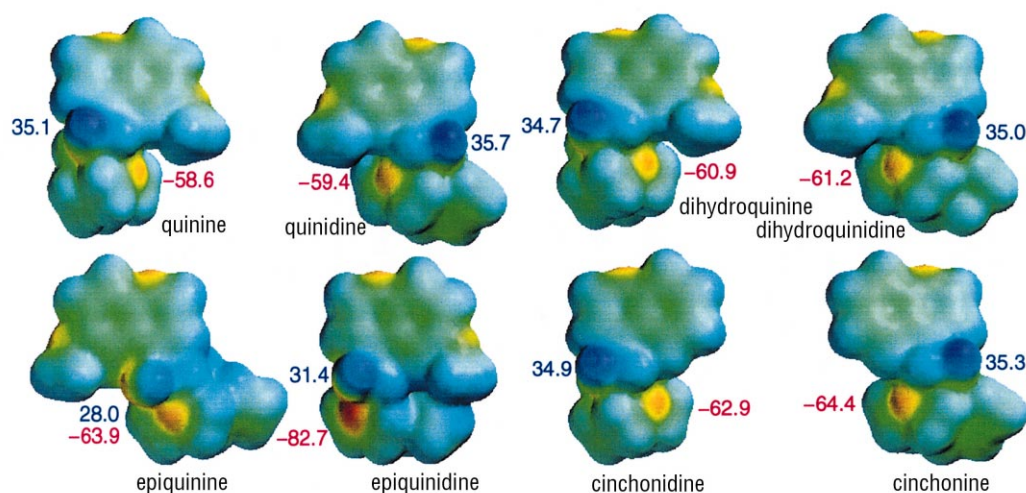


**Figure 3.** Molecular electrostatic potentials plotted onto the total electron density surface (0.002 e/au<sup>3</sup>). The deepest red color corresponds to a potential of −83 kcal/mol, and the deepest blue color corresponds to a potential of 36 kcal/mol. The blue numbers indicate the potential by the hydroxyl hydrogen atom, the most positive site. The red numbers indicate the potential by the aliphatic nitrogen atom. The molecules are oriented as shown in Figure 2 such that both the aliphatic nitrogen and hydroxyl protons are visible.

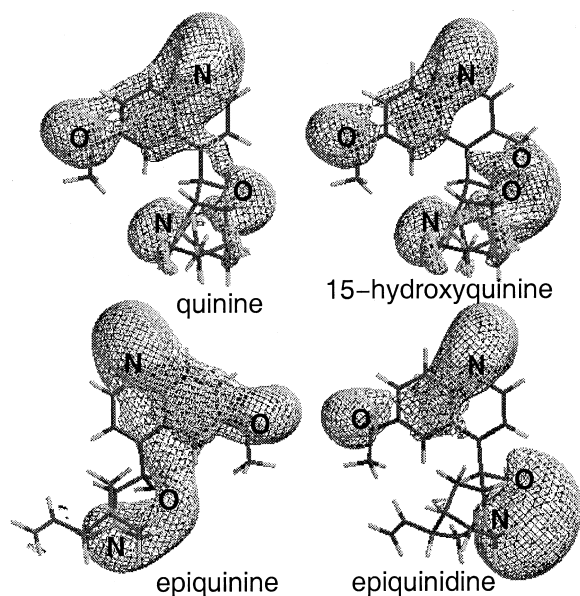


**Figure 4.** Isopotential surfaces. The grid represents a constant potential of  $-10$  kcal/mol. The locations of the heteroatoms are labeled. The isopotential surfaces for all of the other *erythro* cinchona alkaloids are essentially the same as the isopotential surfaces in quinine.

considerable similarity and are represented by quinine in Figure 4. The active *erythro* alkaloids show three distinct negative potential areas: (i) one broad negative potential region extending from the methoxyl oxygen atom to the aromatic ring moiety which covers the quinoline ring, (ii) one negative potential region near the hydroxyl oxygen atom linking the negative potential zone over the quinoline ring through a narrow negative potential pipe, and (iii) an almost isolated, localized potential region by the aliphatic quinuclidine nitrogen atom. In contrast, the  $-10$  kcal/mol isopotential surface of the epiquinine has one extended broad negative potential zone wrapping almost the entire molecule, and in epiquinidine the negative potential wraps around the quinuclidine ring forming a broad bulk engulfing both the hydroxyl and aliphatic amine groups. Thus, it appears from these profiles that the conformation of the epi alkaloids facilitates interaction between the lone pairs of the quinuclidine nitrogen atom, the lone pairs of hydroxyl oxygen atom, and in the case of epiquinine perhaps also with the  $\pi$  system of the quinoline ring. For the active *erythro* alkaloids, the distinct separation of the three negative potential zones enables each region of these alkaloids to interact separately with a receptor and to more readily form hydrogen bonds with a receptor. The diffuse nature of the isopotential surfaces of the epi alkaloids makes recognition by a receptor to specific hydrogen bonding sites more difficult.

#### Highest occupied and lowest unoccupied molecular orbitals (HOMOs and LUMOs)

The molecular orbital energies of the alkaloids were studied in order to assess the alkaloid's reactivity profiles. All of the alkaloids have large negative HOMO energies with relatively smaller negative LUMO energy values (Table 1). This indicates that the electrons are

firmly bound to the nuclei, but that the LUMOs have a strong attraction for electrons. Thus, electron acceptor ability of the alkaloids appears to have a greater role toward antimalarial activity than electron donor ability.

The epi alkaloids have about  $0.25$  eV (about  $6$  kcal/mol) less negative LUMO energy than their *erythro* counterparts. The stronger electron affinity of the epi alkaloids appears to have a negative effect on activity.

#### Proton affinity

The epi alkaloids have on average  $31$  kcal/mol stronger proton affinity of the quinuclidine nitrogen atom than the more active *erythro* alkaloids (Table 1). This suggests a higher  $pK_a$  for protonation of the aliphatic quinuclidine nitrogen atom of the epi alkaloids relative to the *erythro* alkaloids. Thus, the epi alkaloids would have a higher concentration of the protonated form than the *erythro* alkaloids at physiological pH, perhaps resulting in slower diffusion through cell membranes to the site of action.

#### The metabolite 3'-hydroxyquinine

In order to test our results as a predictor of antimalarial activity, the molecular electronic properties of 3'-hydroxyquinine, a major human metabolite of quinine,<sup>24</sup> were calculated. The metabolite is less active in vitro than the *erythro* cinchona alkaloids, but is more active than the epi alkaloids. Specifically, Nonprasert et al.<sup>24</sup> report that 3'-hydroxyquinine is  $4.2$  times less active than quinine against the chloroquine-sensitive D6 *P. falciparum* clone and  $3.4$ – $17.1$  times less active than quinine against four different multi-drug resistant *P. falciparum* patient isolates. The optimized geometry of 3-hydroxyquinine is similar to the *erythro* alkaloids with the  $N1 \cdots O12$  distance equal to  $3.14$  Å, the  $N1 \cdots C5'$  distance equal to  $3.92$  Å, and the  $H8-C8-C9-H9$  dihedral angle equal to  $-81.0^\circ$ .

The molecular electronic properties of 3'-hydroxyquinine are a mixture of the properties of the active and inactive alkaloids (Table 1), consistent with 3'-hydroxyquinine possessing an intrinsic antimalarial activity in-between the activity of the active *erythro* alkaloids and the inactive epi alkaloids. The values for the most negative potential, the negative potential by the aliphatic nitrogen atom, and the HOMO eigen value fall in the range of the active alkaloids. In addition, the LUMO eigen value is more negative than the epi alkaloids. However, the direction of the dipole moment differs from the more potent alkaloids, and the positive potential by the C9 hydroxyl proton is low. The site of the most positive potential moved to the C3 hydroxyl proton with a value of  $49.0$  kcal/mol. The isopotential surface at  $-10$  kcal/mol displayed distinct regions about the quinoline ring and the aliphatic nitrogen atom similar to the more active *erythro* alkaloids, but the negative potential by the C9 hydroxyl group merged with the negative potential by the aromatic C3' hydroxyl group making intermolecular hydrogen bond formation with the C9 hydroxyl group less favorable.

## Conclusion

The most potent cinchona alkaloids possess the following electronic profile: dipole moment magnitude of 2.2 Debye or less, an electric field pointing from the aliphatic nitrogen atom towards the aromatic ring, distinct  $-10$  kcal/mol isopotential surfaces by the quinoline ring and the hydroxyl and aliphatic amine groups, an acidity corresponding to at least  $34.7$  kcal/mol of positive potential by the hydroxyl proton, a basicity of no more negative than  $-64.4$  kcal/mol of negative potential by the aliphatic nitrogen atom, a proton affinity of the aliphatic quinuclidine nitrogen atom of  $200 \pm 5$  kcal/mol, and a comparatively moderate electron affinity. The quinine metabolite shows that having only some of these profile features is insufficient for high antimalarial activity.

The electronic profile thus associated with antimalarial potency of these alkaloids should be useful in the designing of new antimalarial agents, particularly when these results are combined with the electronic profile of other active synthetic aromatic carbinolamine antimalarial agents. The electronic profile for potent activity of the cinchona alkaloids has similarities to a recent stereoelectronic study of mefloquine analogues where the compounds with the most potent antimalarial activity possessed a positive potential by the hydroxyl hydrogen atom of at least  $36$  kcal/mol and a negative potential by the aliphatic nitrogen atom no more negative than  $-64$  kcal/mol, a HOMO eigen value more negative than  $-8.8$  eV, and a LUMO eigen value more negative than  $-0.5$  eV.<sup>25</sup> Potent synthetic non-phenanthrene carbinolamines are also similar with a positive potential by the hydroxyl hydrogen atom of at least  $35.4$  kcal/mol and a negative potential by the aliphatic nitrogen atom no more negative than  $-64.2$  kcal/mol, a HOMO eigen value more negative than  $-9.1$  eV, and a LUMO eigen value more negative than  $-1.2$  eV.<sup>26</sup> Taken together these results provide a set of electronic properties evidently necessary for antimalarial potency.

The stereoelectronic profiles of the cinchona alkaloids may also be helpful in understanding why the proteolipid subunit of the  $F_0 F_1 H^+$ -ATPase of *Streptococcus pneumoniae* is inhibited by quinine and quinidine, but not by epiquinine and epiquinidine.<sup>27</sup> In all likelihood, the epi alkaloids are not able to bind to the ATPase in the same manner as quinine and quinidine.

The stereoelectronic features of the cinchona alkaloids increases our understanding of their mechanism of action at the molecular level by showing that both steric and electronic factors appear to be affecting the hydrogen bonding capacity of the inactive *epi* alkaloids. A previous crystallographic study<sup>13</sup> demonstrated that the conformational differences between the *erythro* and the *threo* alkaloids forces the direction of hydrogen bonding between the alkaloid and a receptor to differ. In other words, the *epi* alkaloids cannot form hydrogen bonds from the hydroxyl and the aliphatic amine groups with the same geometry as the *erythro* alkaloids. Likewise, the electronic profiles of the less active quinine

metabolite and the inactive *epi* alkaloids are less favorable for facile intermolecular bond formation between a receptor and the hydroxyl and amine groups of the alkaloid. This results from the lower magnitude of the electrostatic potential by the hydroxyl group and the diffuse negative isopotential surfaces which reduce the recognition of the receptor with specific hydrogen bonding sites. Thus, for both steric and electronic reasons, the *threo* epi alkaloids cannot hydrogen bond to a receptor in the same manner as the potent *erythro* alkaloids. This may be crucial to the antimalarial activities of the cinchona alkaloids.

## Experimental

### Geometry optimization and energy calculations

Geometry optimization and energy calculations were performed on the free base and protonated forms of each alkaloid at the ab initio quantum chemical level by using the 3-21G split-valence basis set as implemented in the Gaussian 94 package<sup>28</sup> running on a Silicon Graphics Power Indigo R8000 workstation. The starting geometry for optimization of the *erythro* alkaloids was taken from the crystal structures of quinine and quinidine<sup>14,15</sup> and for the *threo* epi alkaloids from their reported crystal structures.<sup>13,16</sup> Geometry optimization and electrostatic potential profiles of the molecules were determined in the presence of an aqueous environment in order to simulate biological environments. The effects of aqueous solvation were calculated using the self-consistent reaction field (SCRF) method by Dixon,<sup>29</sup> a modification of the Onsager Model.<sup>30–32</sup> In this method, the aqueous solvent is viewed as a continuum medium of uniform dielectric constant. The dipole in the molecule induces a dipole in the aqueous medium generating an electric field which in turn interacts with the molecular dipole creating an additional term in the Hamiltonian for the solvent effect.

### Calculation of molecular electronic properties

The molecular electronic properties of the compounds such as dipole moment, molecular electrostatic potentials, and molecular orbital energies were calculated on the optimized geometries of the molecules using SPARTAN software<sup>33</sup> running on a Silicon Graphics Indigo Extreme R4000 workstation. The molecular electrostatic potential in the range from  $-83.0$  to  $36.0$  kcal/mol was superimposed onto a surface of constant electron density ( $0.002 \text{ e}/\text{au}^3$ ) to provide a measure of the electrostatic potential at roughly the van der Waals surface of the molecule. This color-coded surface provides a measure of the overall size of the molecule as well as the location of the positive (deepest blue, most positive) and negative (deepest red, most negative) electrostatic potentials. The regions of positive electrostatic potential indicate excess positive charge, that is, repulsion of the positively charged test probe, while regions of negative potential indicate areas of excess negative charge, that is, attraction of the positively charged test probe. Three-dimensional surfaces of molecular electrostatic potential

at a constant  $-10$  kcal/mol were generated to provide a profile of the electrostatic potential encountered by an approaching molecule.

### Proton affinity

Proton affinity (PA) of the aliphatic quinuclidine nitrogen atom was calculated using the equation  $PA = \Delta H_f(H^+) + \Delta H_f(B) - \Delta H_f(BH^+)$ , where  $\Delta H_f(H^+)$  is equal to 367.2 kcal/mol, the experimentally determined value of the heat of formation of a free proton,<sup>34</sup> where  $\Delta H_f(B)$  is the calculated heat of formation of the free base form of the alkaloid, and where  $\Delta H_f(BH^+)$  is the calculated heat of formation of the alkaloid protonated at the aliphatic nitrogen atom.

### Antimalarial activity

Structure–activity relationships are based upon in vitro *P. falciparum* assay results<sup>13,24</sup> using the chloroquine-sensitive Sierra Leone D-6 clone and the chloroquine-resistant Indochina W-2 clone. The  $IC_{50}$  values for quinine, dihydroquinine, quinidine, dihydroquinidine, epiquinine, and epiquinidine were obtained from ref. 13, the  $IC_{50}$  values for cinchonine and cinchonidine were obtained from the Department of Parasitology, Walter Reed Army Institute of Research, and the  $IC_{50}$  value for 3'-hydroxyquinine was obtained from ref. 24 and normalized using the  $IC_{50}$  value for quinine in ref. 13.

### Acknowledgements

The authors thank Dr. Dennis Kyle and Ms. Lucia Gerena of the Department of Parasitology, Division of Experimental Therapeutics, Walter Reed Army Institute of Research, for the  $IC_{50}$  values for cinchonine and cinchonidine. We also thank the National Research Council, Washington, DC, for their support of Dr. Bhattacharjee.

### References

1. Tracy, J. W.; Webster, L. T. In *The Pharmacological Basis of Therapeutics*; Hardman, J. G.; Limbird, L. E.; Molinoff, P. B.; Ruddon, R. W.; Gilman, A. G., Eds.; McGraw-Hill: New York, 1993, 9th ed., pp 965–985.
2. White, N. J. *Eur. J. Clin. Pharmacol.* **1988**, *34*, 1.
3. White, N. J.; Hien, T. T. *Bull. Trop. Med. Intl. Health* **1993**, *1*, 2.
4. Meshnick, S. R. In *Malaria: Parasite Biology, Pathogenesis, and Protection*; Sherman, I. W., Ed.; ASM Press: Washington, D.C., 1998, pp 341–353.
5. Olliaro, P. L.; Goldberg, D. E. *Parasitol. Today* **1995**, *11*, 294.
6. Panisko, D. M.; Keystone, J. S. *Drugs* **1990**, *39*, 160.

7. Schlesinger, P. H.; Krogstad, D. L.; Herwaldt, B. L. *Antimicrob. Agents Chemother.* **1988**, *32*, 793.
8. Slater, A. F. G.; Cerami, A. *Nature* **1992**, *355*, 167.
9. Blierer, D. E.; Dener, J. M.; Dubenko, L. G.; Gerber, R. E.; Litvak, J.; Peterli, S.; Peterli-Roth, P.; Truong, T. V.; Mao, G.; Bauer, B. E. *J. Med. Chem.* **1995**, *38*, 2628.
10. Ganellin, C. R.; Mitchell, R. C.; Young, R. C. In *Recent Advances in Receptor Chemistry*; Melchiorre, C.; Giannella, M., Eds.; Elsevier Science Publishers B.V.: Amsterdam, 1988, pp 289–306.
11. Guha, S.; Majumdar, D.; Bhattacharjee, A. K. *J. Mol. Structure (Theochem.)* **1992**, *256*, 61.
12. Sjoberg, P.; Murray, J. S.; Brinck, T.; Evans, P.; Politzer, P. *J. Mol. Graphics* **1990**, *8*, 81.
13. Karle, J. M.; Karle, I. L.; Gerena, L.; Milhous, W. K. *Antimicrob. Agents Chemother.* **1992**, *36*, 1538.
14. Karle, I. L.; Karle, J. *Proc. Natl. Acad. Sci. USA* **1981**, *78*, 5938.
15. Pniewska, B.; Suszko-Purycka, A. *Acta Crystallogr.* **1989**, *C45*, 638.
16. Karle, J. M.; Karle, I. L. *Acta Crystallogr.* **1992**, *C48*, 1975.
17. Doherty, R.; Benson, W. R.; Maienthal, M.; McD Stewart, J. *J. Pharmaceut. Sci.* **1978**, *67*, 1698.
18. Kashino, S.; Haisa, M. *Acta Crystallogr.* **1983**, *C39*, 310.
19. Oleksyn, B. *Acta Crystallogr.* **1982**, *B38*, 1832.
20. Oleksyn, B.; Lebiada, L. *Acta Crystallogr.* **1979**, *B35*, 440.
21. Dijkstra, G. D. H.; Kellogg, R. M.; Wynberg, H. *Recl. Trav. Chim. Pays-Bas* **1989**, *108*, 195.
22. Dijkstra, G. D. H.; Kellogg, R. M.; Wynberg, H.; Svendsen, J. S.; Marko, I.; Sharpless, K. B. *J. Am. Chem. Soc.* **1989**, *111*, 8069.
23. Kumar, A.; Bhattacharjee, A. K.; Mishra, P. C. *Intl. J. Quant. Chem.* **1992**, *43*, 579.
24. Nonprasert, A.; Pukrittayakamee, S.; Kyle, D. E.; Vanijanonta, S.; Kyle, N. J. *Trans. Royal Soc. Trop. Med. Hyg.* **1996**, *90*, 553.
25. Bhattacharjee, A. K.; Karle, J. M. *J. Med. Chem.* **1996**, *39*, 4622.
26. Bhattacharjee, A. K.; Karle, J. M. *Bioorg. Med. Chem.* **1998**, *6*, 1927.
27. Munoz, R.; Garcia, E.; de la Campa, A. G. *J. Bacteriol.* **1996**, *178*, 2455.
28. Frisch, M. J.; Trucks, G. W.; Schlegel, H. B.; Gill, P. M. W.; Johnson, B. G.; Robb, M. A.; Cheeseman, J. R.; Keith, T. A.; Petersson, G. A.; Montgomery, J. A.; Raghavachari, K.; Al-Laham, M. A.; Zakrzewski, V. G.; Ortiz, J. V.; Foresman, J. B.; Cioslowski, L.; Stefanov, B. B.; Nanayakkara, A.; Challacombe, M.; Peng, C. Y.; Ayala, P. Y.; Chen, W.; Wong, M. W.; Andres, J. L.; Replogle, E. S.; Gomperts, R.; Martin, R. L.; Fox, D. J.; Binkley, J. S.; Defrees, D. L.; Baker, J.; Stewart, J. P.; Head-Gordon, M.; Gonzalez, C.; Pople, J. A. *Gaussian 94* (Revision A.1). Gaussian, Inc., Pittsburgh, PA, 1995.
29. Dixon, R. W.; Leonard, J. M.; Hehre, W. J. A. *Israel J. Chem.* **1993**, *33*, 427.
30. Alagona, G.; Ghio, C. *J. Mol. Struct. (Theochem.)* **1992**, *256*, 187.
31. Luque, F. J.; Gadre, S. R.; Orozco, M.; Bhadane, P. K. *J. Phys. Chem.* **1993**, *97*, 9380.
32. Wong, M. W.; Frisch, M. J.; Wiberg, K. B. *J. Am. Chem. Soc.* **1991**, *113*, 4776.
33. SPARTAN version 4.0, Wavefunction, Inc., Irvine, CA.
34. Dewar, M. J. S.; Dieter, K. M. *J. Am. Chem. Soc.* **1986**, *108*, 8075.